Use of color maps and wavelet coherence to discern seasonal and interannual climate influences on streamflow variability in northern catchments

Sean K. Carey,[1] Doerthe Tetzlaff,[2] Jim Buttle,[3] Hjalmar Laudon,[4] Jeff McDonnell,[5] Kevin McGuire,[6] Jan Seibert,[7] Chris Soulsby,[2] and Jamie Shanley[8]

Received 6 August 2012; revised 3 August 2013; accepted 10 August 2013.

[1] The higher midlatitudes of the northern hemisphere are particularly sensitive to change due to the important role the 0°C isotherm plays in the phase of precipitation and intermediate storage as snow. An international intercatchment comparison program called North-Watch seeks to improve our understanding of the sensitivity of northern catchments to change by examining their hydrological and biogeochemical variability and response. Here eight North-Watch catchments located in Sweden (Krycklan), Scotland (Girnock and Strontian), the United States (Sleepers River, Hubbard Brook, and HJ Andrews), and Canada (Dorset and Wolf Creek) with 10 continuous years of daily precipitation and runoff data were selected to assess daily to seasonal coupling of precipitation (P) and runoff (Q) using wavelet coherency, and to explore the patterns and scales of variability in streamflow using color maps. Wavelet coherency revealed that P and Q were decoupled in catchments with cold winters, yet were strongly coupled during and immediately following the spring snowmelt freshet. In all catchments, coupling at shorter time scales occurred during wet periods when the catchment was responsive and storage deficits were small. At longer time scales, coupling reflected coherence between seasonal cycles, being enhanced at sites with enhanced seasonality in P. Color maps were applied as an alternative method to identify patterns and scales of flow variability. Seasonal versus transient flow variability was identified along with the persistence of that variability on influencing the flow regime. While exploratory in nature, this intercomparison exercise highlights the importance of climate and the 0°C isotherm on the functioning of northern catchments.

Citation: Carey, S. K., D. Tetzlaff, J. Buttle, H. Laudon, J. McDonnell, K. McGuire, J. Seibert, C. Soulsby, and J. Shanley (2013), Use of color maps and wavelet coherence to discern seasonal and interannual climate influences on streamflow variability in northern catchments, *Water Resour. Res.*, *49*, doi:10.1002/wrcr.20469.

1. Introduction

[2] Exploring relations between precipitation and runoff response has formed the basis of hydrological analysis for nearly a century and there is a continuing interest in understanding how precipitation is transferred toward the stream network and routed to the catchment outlet. Applications such as flood forecasting and reservoir management that have societal relevance have delivered several empirical relations now used in prediction [e.g., *Wilcox et al*., 1990; *Beven*, 2001; *Lyon et al*., 2004], while concurrent basic research on input-output relations has led to new understanding of catchment functioning, storage dynamics, and biogeochemical cycling [e.g., *Tetzlaff et al*., 2007; *Laudon et al*., 2011; *McNamara et al*., 2011; *Sayama et al*., 2011].

[3] Recent catchment-scale work has focused on the coupling of precipitation (P) and discharge (Q) and the link between storage and discharge (including threshold responses) as a unifying concept for catchment response [e.g., *Kirchner*, 2009; *Ali et al*., 2011; *Peters and Aulenbach*, 2011; *Shook and Pomeroy*, 2011]. In this framework, catchments must exceed a moisture threshold to become

[1]School of Geography and Earth Sciences, McMaster University, Hamilton, Ontario, Canada.
[2]School of Geosciences, Northern Rivers Institute, University of Aberdeen, Aberdeen, Scotland.
[3]Department of Geography, Trent University, Peterborough, Ontario, Canada.
[4]Forest Ecology and Management, Swedish University of Agricultural Sciences, Uppsala, Sweden.
[5]School of Environment and Sustainability, University of Saskatchewan, Saskatoon, Saskatchewan, Canada.
[6]Virginia Water Resources Research Center and Department of Forest Resources and Environmental Conservation, Virginia Tech, Blacksburg, Virginia, USA.
[7]Department of Geography, University of Zurich, Zurich, Switzerland.
[8]U.S. Geological Survey, Montpelier, Vermont, USA.

Corresponding author: S. K. Carey, School of Geography and Earth Sciences, McMaster University, Hamilton, ON L8S 4L8, Canada. (careysk@mcmaster.ca)

0043-1397/13/10.1002/wrcr.20469

responsive to inputs, with soil, bedrock topography, and catchment morphometry all being identified as important first-order controls on this relationship [*Tromp-van Meerveld and McDonnell*, 2006; *Spence*, 2007; *Detty and McGuire*, 2010]. The temporal pattern of this coupling is controlled by both intrinsic and extrinsic factors, and a system "memory" exists whereby P-Q coupling has discernible temporal patterns and cycles that persist intra and interannually, and over decadal scales in response to global linkages [*Keener et al*., 2010; *Niedzielski*, 2011; *Ouachani et al*., 2013]. Catchment soils, geology, topology, and topography all influence catchment storage and short-term responses to water balance dynamics [*Buttle*, 2006], whereas climate imparts a periodicity in hydrological patterns when observed at seasonal, annual, and decadal scales. For example, catchments with thin soils and little storage capacity have inherently little memory of past inputs, rapidly translating precipitation to runoff with limited threshold response behavior. In contrast, catchments with large storage capacity have greater memory of past inputs as streamflow variability is dampened during filling of soil and surface reservoirs after dry periods.

[4] Climate affects the temporal occurrence of hydrological patterns as catchments with strong seasonal precipitation cycles have considerable regularity of high and low flow periods, whereas catchments with a more uniform precipitation and/or P-evaporation (E) have less. Over longer time scales, streamflow patterns are linked to global patterns of pressure and sea surface temperature, which affect regional climate variability at continental scales [e.g., *Foley et al*., 2002; *Ionita et al*., 2012]. The 0°C isotherm threshold, defined in time as the occurrence when air temperature crosses the freezing point of water (in this paper taken on a daily basis), further affects the regularity of response as catchments that accumulate snow and develop frozen ground have a hydrological response largely governed by the timing and magnitude of snowmelt or ground thaw. To date, few P-Q studies have included specific analyses of snowmelt-dominated systems, and there remains a lack of insight into fundamental questions in these systems related to moisture thresholds for flow generation, modulation by soil depth and frozen ground, bedrock topography, catchment morphometry, and how short and longer-term climate drivers may influence streamflow variability in northern catchments.

[5] In this paper, we explore the coupling of P and Q and the nature of variability among mid high-latitude catchments with partial or seasonal snowcover within an intercomparison framework. We go beyond the traditional metrics of streamflow patterns and hydrograph characteristics [as used by *Richter et al*., 1998; *Clausen and Biggs*, 2000; *Archer and Newson*, 2002; *Olden and Poff*, 2003; *Monk et al*., 2011], employing alternate techniques to analyze synchrony and coupling of P and Q signals across daily to seasonal time scales [following *Jones*, 2005; *Carey et al*., 2010]. Specifically, we use color maps and wavelet coherence to discern daily to seasonal climate influences on streamflow variability on eight northern watersheds that are part of the North-Watch intercomparison program (http://abdn.ac.uk/northwatch). Color maps are simple tri-dimensional plots with time on the *x* axis, period on the *y* axis, and the quantity of interest (z) represented by colors in 2-D space [*Meko et al*., 2012]. Wavelet analysis (see *Torrence and Compo* [1998] for an introduction) is gaining widespread application in hydrology to both identify the scale and timing of temporal patterns in a time series, and to identify periods of coherence between two time series [e.g., *Lafreniere and Sharp*, 2003; *Kang and Lin*, 2007; *Keener et al*., 2010; *Wörman et al*., 2010; *Mengistu et al*., 2013]. Wavelet coherency [*Liu*, 1994; *Grinsted et al*., 2004], which compares two wavelet spectra, allows identification of scales and times when time series (such as P and Q) are experiencing oscillations at a similar frequency of interest and are in effect coupled.

[6] The North-Watch program explores climate, hydrology, and ecology data sets from high-latitude experimental catchments with long histories of process-based research spanning different hydro-climatic zones within Scotland, Canada, Sweden, and the United States [*Tetzlaff et al*., 2013]. *Carey et al*. [2010] utilized 10 years of daily precipitation, runoff, temperature, and storage change data along with topographic information to group catchments into those that exhibited greater hydrological resistance (i.e., those catchments that were more or less hydrologically responsive to inputs) and resilience to change (i.e., those that were able to return to normal function after perturbation). Important factors that characterized different catchment types were the synchrony (the degree to which cycles are in phase) between the seasonal variability of P and Q, and where catchments mapped on a gradient of warm/wet versus cool/dry.

[7] To further understanding the nature of variability in catchments that are seasonally snow covered along a hydrometric gradient, the specific objectives of this paper are to:

[8] 1. Assess the influence of short-term and transient events versus seasonal climate signals in the flow regime using variance visualization (color maps) and

[9] 2. Explore the coupling of precipitation and discharge at daily to seasonal scales using wavelet coherency analysis.

[10] By focusing on the variability in runoff as opposed to magnitudes or other more common flow metrics, we seek to establish at what periods, climate forcing results in regularity and irregularity in flows. We further hypothesize that wavelet coherency analysis [*Liu*, 1994; *Torrence and Compo*, 1998] will highlight periods of P-Q synchrony, and help identify climate and catchment factors influencing synchrony. By comparing variability and coupling among catchments, similarities and differences in patterns can be observed and linked to our process understanding of these systems. This will help to identify the appropriate focal length for precipitation-discharge relationship investigations, which is particularly important for northern regions where measurements are often difficult.

2. Study Sites

[11] Eight of the 10 North-Watch catchments were used for this analysis as they had a complete 10 year temperature, precipitation, and discharge data set, although the 10 year records were not for the same years. These catchments traverse a hydro-climatic gradient and span a range of geological and edaphic conditions (Figure 1) and have been described previously by *Carey et al*. [2010] and *Kruitbos*

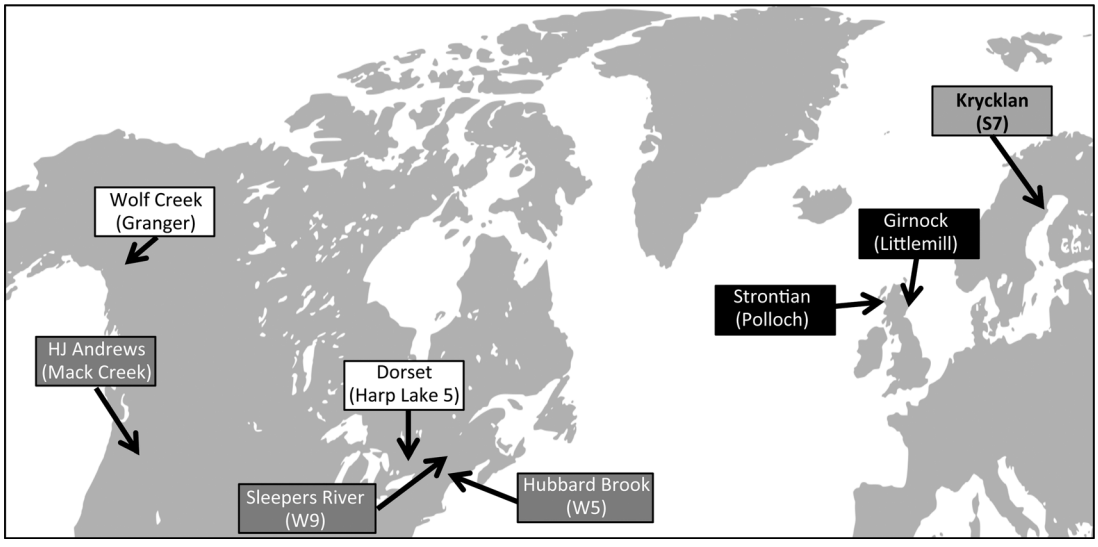

Figure 1. Location of eight selected North-Watch catchments. Text in brackets denotes the subcatchment for which data were obtained.

et al. [2012]. Two catchments are located in Scotland (Girnock, Strontian), two in Canada (Dorset, Wolf Creek), three in the United States (HJ Andrews, Hubbard Brook, Sleepers River), and one in Sweden (Krycklan). Catchment physical characteristics and hydro-climatic regime are summarized in Table 1.

[12] The two Scottish catchments are distinct. Strontian (9 km^2) is warm (mean annual air temperature (MAAT) of 9.1°C) and the wettest of all, and its geology is predominantly schist, and gneiss with volcanic and sedimentary material overlain with thin hydrologically responsive soils [*Hrachowitz et al*., 2010]. Girnock (30 km^2) is cooler (MAAT of 6.7°C) with approximately half the precipitation of Strontian and is characterized by igneous granite with superficial drifts. Peats and gley soils are dominant in valley bottoms and gentle slopes [*Tetzlaff et al*., 2007]. Strontian is partly forested, whereas Girnock is unforested with moorland vegetation.

[13] Wolf Creek (7.6 km^2, Granger subbasin), on the fringe of the Coast Mountains, Yukon Territory, Canada, is the coldest (MAAT of −2.2°C) and driest (478 mm) catchment. Its geology is sedimentary with a till mantle of varying depths overlain by organic soils at lower elevations. Permafrost (perennially frozen ground) underlies approximately 70% of the basin. The catchment is above tree line and is dominated by willow and birch shrubs at lower elevation and tundra at higher elevation. The second Canadian site is Dorset (1.9 km^2, Harp Lake 5), in the southern Boreal ecozone of south-central Ontario. MAAT is 4.9°C with precipitation of 980 mm evenly distributed throughout the year. Bedrock is predominantly Precambrian shield and is overlain by a thin layer of till. Forests are a mix of deciduous and conifer species.

[14] Two catchments in the United States that lie within a similar, yet wetter, hydro-climatic region to Dorset are Sleepers River and Hubbard Brook. Sleepers River (0.41 km^2, W9) is wetter (1256 mm) than Dorset with a bedrock of quartz-mica phyllite with beds of calcareous granulate overlain by dense silty glacial till. Inceptisols and Spodosols overlie the till to an average depth of 0.7 m with Histosols in riparian zones. Vegetation is mostly northern hardwoods [*Shanley et al*., 2004]. Hubbard Brook (0.41 km^2, WS3) has a similar climate to Sleepers River [*Bailey et al*., 2003]. MAAT is 6.4°C with 1361 mm of precipitation. Bedrock is composed of olitic schist overlain by basal and ablation tills. Approximately 80% of the soils are Spodosols and 20% Inceptisols. The catchment is entirely forested with second-growth northern hardwoods. The third United States catchment is HJ Andrews (5.8 km^2, Mack Creek) in the western Cascades of Oregon. It is the warmest (MAAT of 9.2°C) North-Watch catchment and the steepest with 860 m of relief. Precipitation exceeds 2000 mm and is concentrated in the winter. Geology is composed of andesitic and basaltic lava flows and soils are deeply weathered and freely draining [*Dyrness*, 1969; *Swanson and James*, 1975]. The catchment was not glaciated and is covered by coniferous forests [*McGuire et al*., 2005].

[15] Krycklan (0.5 km^2, S7) is the Swedish site located on the Fennoscandian shield [*Laudon et al*., 2011] and is the second driest (651 mm) and second coldest catchment (MAAT of 2.4°C). Geologically, it is underlain by metasediments with podzol soils. Coniferous forests predominate throughout the catchment.

3. Methods

3.1. Data Set

[16] Ten years of continuous daily air temperature, precipitation, and streamflow data were used for each of the catchments. Considerable effort was undertaken to standardize and quality control the data sets, forming a unique high accuracy data resource across the mid- and high-latitude northern region. The method of data collection varied among catchments, and temperature and precipitation were acquired from national weather networks at most sites, supplemented by local observations. Precipitation as snow was directly measured, yet the timing and rate of melt was not available at most sites. To obtain a

Table 1. Site Characteristics of the North-Watch Study Catchments

Country	Catchment	Site	Area (km^2)	Wetland Cover (%)	Mean Altitude (m)	Relief (m)	Dominant Geology	Dominant Land Cover	Temperature (°C)	Precipitation {% Snow} (mm)	Runoff (mm)
Scotland	Girnock	Littlemill	30	18	405	620	Granite	Moorland/Peat	6.73	1059 {10}	603
	Strontian	Polloch	8	0	340	740	Schist, Gneiss	Moorland	9.08	2632 {4}	2213
	Dorset	Harp Lake 5	1.9	13.3	373	93	Metamorphic	Forest/Peat	4.94	980 {28}	577
Canada	Wolf Creek	Granger Basin	7.6	<5	1700	750	Metasediments	Shrub/subalpine Alpine/Tundra	−2.15	478 {45}	352
Sweden	Krycklan	S7	0.5	15	280	72	Metasediments	Forest, Wetland	2.41	651 {40}	327
USA	HJ Andrews	Mack Creek	5.81	0	1200	860	Igneous	Forest	9.22	2158 {40}	1744
	Hubbard Brook	W3	0.41	0	642	210	Igneous/Metamorphic	Northern Hardwood	6.41	1381 {25}	882
	Sleepers River	W9	0.41	5	604	167	Metasediments	Forest	4.66	1256 {25}	743

comparable data set that reflects the hydrological inputs, a degree-day melt model was applied [*Gray and Male*, 1981]. At temperatures <0°C, all precipitation was accumulated as snow. When temperatures were >0°C, P was rain plus any accumulated snowmelt on a daily basis using a melt factor of 4 mm/°C/day. While this approach is simple, in the absence of energy-balance data and direct observations for such a cross-comparison study, it provides a first-order estimate of actual water input to the sites.

3.2. Variability Analysis

[17] The most common measure of expressing temporal variability in a data set is through describing the dispersion of a probability distribution. In hydrology, metrics such as standard deviation (SD) and the normalized coefficient of variation (CV) along with more robust measures such as the interquartile range (IQR) are commonly used to describe population dispersions and visualized with classical graphical techniques such as box-and-whisker diagrams (Figure 2). There has been less attention paid to the temporal nature of dispersion, and few examples consider how dispersion persists in a time series. Here we present a color map method of displaying the dispersion of daily flows. This approach is similar to that of *Meko et al*. [2012] who applied color maps of mean annual flows over an averaging period of several hundred years. Analytically, dispersion metrics were calculated from the 10 years of record. For each day of the 10 years of daily flow observations, a m-day running mean was computed for $m = 1,2,\ldots,30$ days centered on the day in question. This generated time series with progressively averaged flow data, for which the variability statistics (SD, CV, and IQR) were calculated for each point on the matrix. A two-dimensional surface was then generated by plotting the dispersion statistic for the day of year (x axis), which is the central day of the m-day average, against the m day averaging period (y axis) of the progressively smoothed time series. The averaging period (displayed up to 30 days) shows the temporal persistence of variability in flow. The scale for daily runoff (dots) is displayed on the right-hand y axis.

[18] We explored several methods of displaying patterns of spatial variability using the above techniques, and each provides its own strengths and weaknesses for intercomparison among sites. SD is biased by the magnitude of discharge as catchments with greater flows have greater SD on a given day (as would be expected) and by extreme events as one very high flow can have notable influence on the color map. Plotting CV as the dispersion metric strongly emphasized variability in low flow periods, which although useful to identify periods of unexpected flows during base flow, did not reflect actual magnitudes of flow variability (see *Tetzlaff et al*. [2013] for color maps of CV). To reduce the considerable influence of outlier high flows while still reflecting the overall pattern of variability, the IQR normalized by the global mean flow was used. Normalizing by the global mean 10 year flow for each catchment allows plotting on a common scale for intercomparison, whereas the IQR represents the centroid of the dispersion without the influence of extreme events.

3.3. Wavelet Coherence Analysis

[19] Hydrological time series are rarely stationary, consisting of a variety of frequency regimes that may be

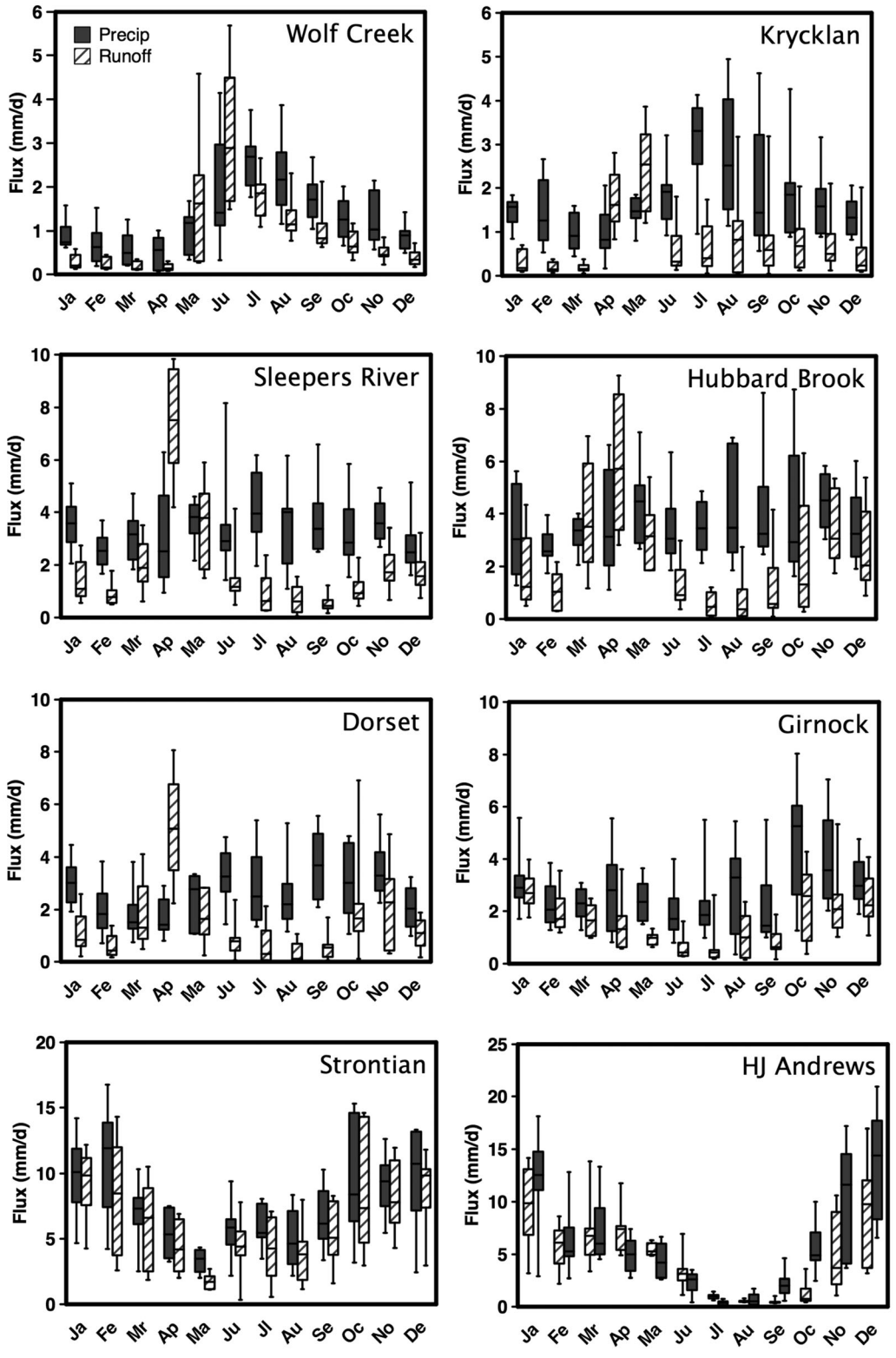

Figure 2. Ten year box-and-whisker monthly precipitation and runoff for the study sites. Whiskers extend to the 10th and 90th percentile. Precipitation is displayed as recorded at the site.

localized in space or span a large portion of the temporal record [e.g., *Kondrashov et al*., 2005; *Burn*, 2008]. These patterns in the time series reflect important parts of the hydrological cycle, particularly at intra-annual time scales. Wavelet analysis provides a method to examine these localized patterns and transient features of the hydrological cycle [*Torrence and Compo*, 1998; *Lafreniere and Sharp*, 2003; *Grinsted et al*., 2004; *Labat*, 2005, 2008; *Kang and Lin*, 2007; *Guan et al*., 2011; *Mengistu et al*., 2013]. Wavelet transforms surpass Fourier transforms, which lose

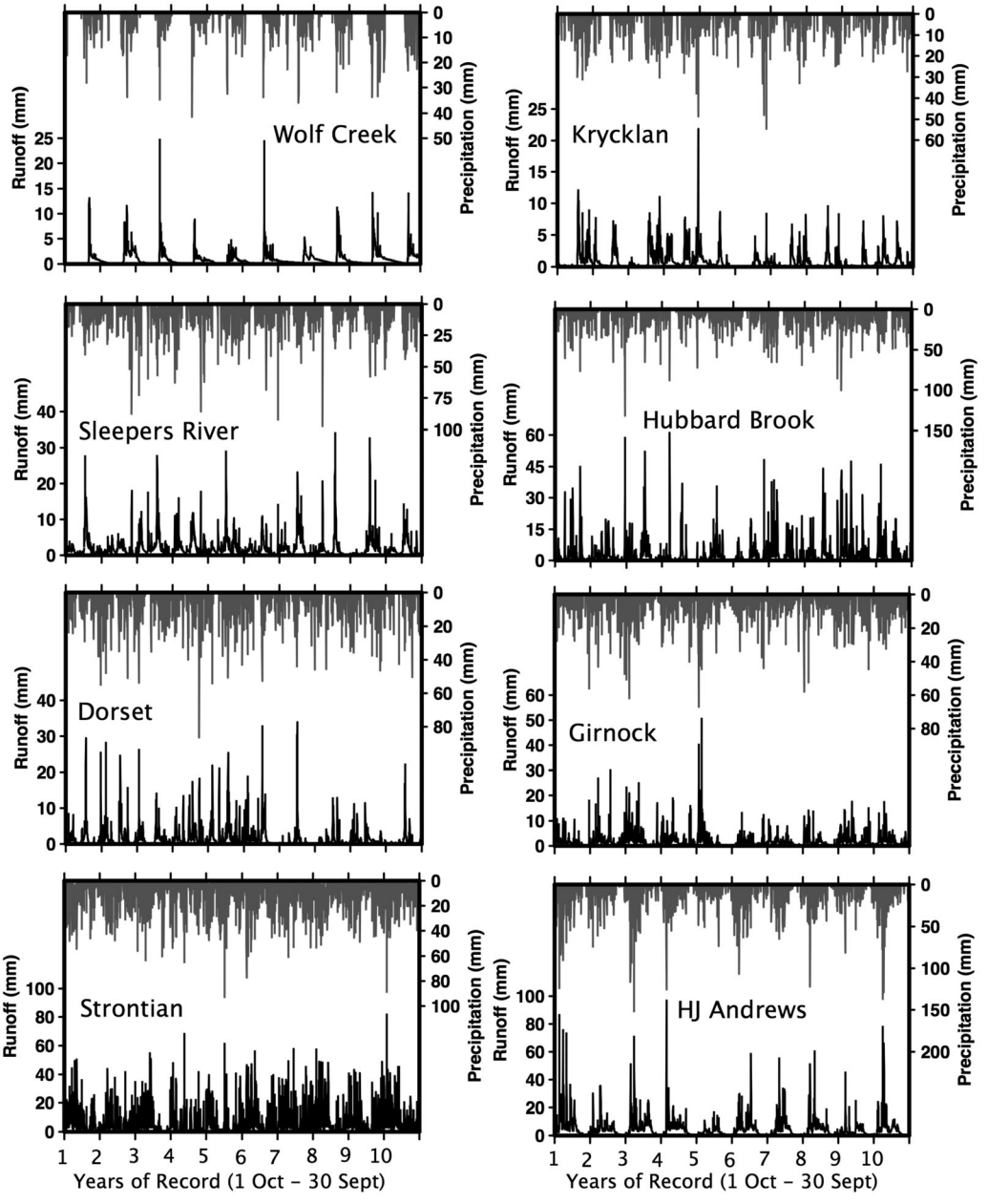

Figure 3. Ten year record of precipitation (top gray bars) and discharge (bottom black line) for the study sites. Precipitation is displayed as input to catchment using rainfall plus the degree-day method for snowmelt.

information as they separate variances at different scales [*Si*, 2008], whereas Fourier transforms surpass the wavelet transform in the frequency location of the variance. The wavelet transform enables examination of time series features at scales locally with details matched by their scale (e.g., broad features at long time scales and fine features at short ones). This property is particularly useful for time series with temporal variations that are nonstationary, have short-lived transient components and features at different scales, or have singularities.

[20] Here to assess synchrony and coupling between precipitation and runoff, the covariation of the power spectra of P and Q was calculated using the wavelet coherence Matlab package presented in *Grinsted et al*. [2004] (available from http://www.pol.ac.uk/home/research/waveletcoherence/). This approach computes the wavelet power spectra using the Morlet wavelet, which has found widespread application in hydrology due to its frequency resolution and ability to detect both time-dependent amplitude and phase for different frequencies in the time series [*Torrence and Compo*, 1998; *Labat*, 2005; *Soniat et al*., 2006]. It is characterized as:

$$\psi_o(\eta) = \pi^{-\frac{1}{4}} e^{i\omega_0\eta} e^{-\frac{\eta^2}{2}} \quad (1)$$

[21] where $\psi_o(\eta)$is the wavelet function, η is a dimensionless time parameter, i is the imaginary unit, and ω_o dimensionless angular frequency taken as 6 which provides

a balance between time and frequency localization. For a time series X_n for each scale s at all n of series length N, the wavelet function is mathematically represented as:

$$W_n(s) = \frac{1}{N}\sum_{n'=0}^{N-1} x_{n'}\psi * \left[\frac{(\eta' - \eta)\Delta t}{s}\right] \quad (2)$$

[22] where $W_n(s)$ is the wavelet transform coefficients, ψ the normalized wavelet, $(^*)$ the complex conjugate, s the wavelet scale, n the localized time index, and n' the translated time index of the time ordinate x.

[23] The wavelet coherence is analogous to the correlation coefficient between two series in the frequency domain and for two time series X and Y with wavelet transforms $W_n^X(s)$ and $W_n^Y(s)$ is defined as:

$$R_n^2(s) = \frac{\left|S\left(s^{-1}W_n^{XY}(s)\right)\right|^2}{S\left(s^{-1}\left|W_n^X(s)\right|^2\right) \times S\left(s^{-1}\left|W_n^Y(s)\right|^2\right)} \quad (3)$$

[24] where S is a smoothing operator both in the scale axis and time domain.

$$S(W) = S_{scale}(S_{time}(W_n(s))) \quad (4)$$

[25] where S_{time} smooths along the time axis and S_{scale} along the scale axis. It is important to note that coherence between two wavelet spectra does not indicate correlation at high power, but that similar oscillations are occurring in each series at the frequency of interest. The null model used for statistical testing was a first-order autoregressive model computed using 1000 random realizations via a Monte Carlo approach, which is typically applied for hydrological and ecological data [*Maraun and Kurths*, 2004; *Rouyer et al*., 2008]. Readers are referred to *Torrence and Compo* [1988]; *Grinsted et al*. [2004]; *Labat* [2005]; and *Si* [2008] for details on the necessary data preparation and further mathematical expressions.

4. Results

4.1. Variability

[26] Monthly P and Q for the 10 year catchment records show considerable variability in their magnitude, timing, and synchrony (Figure 2). Strontian and HJ Andrews are the wettest sites, with Strontian having a much less pronounced wet/dry season differentiation compared with HJ Andrews. In catchments with significant snow storage, spring Q is typically greater than P, largely because P as recorded does not reflect accumulated snow storage, melt, and delayed water delivery. In northeastern North America (Sleepers River, Hubbard Brook, Dorset) and Krycklan, drying soils with increased soil water storage capacity in summer results in a divergence between P and Q, which declines in autumn as evapotranspiration decreases and the ratio of Q/P increases. In wet catchments and those with more uniform distribution of P, the Q/P ratio remains more consistent on a month-to-month basis. Ten years of daily P calculated with the degree-day method and Q highlights the considerable differences in input and output signals among the catchments (Figure 3). Catchments such as Wolf Creek and HJ Andrews have strong annual periodicity in both P and Q, whereas Strontian and Sleepers River have greater variability expressed over shorter periods. While 10 years is too short of a period to assess changes and trends in P or Q regimes, Dorset has considerably less flow and variability after year 7 than the early period of record.

4.1.1. Color Maps

[27] Flow normalized color maps of IQR are presented in Figure 4. Wolf Creek has both flow and variability dominated by the magnitude and timing of spring melt during early May through mid June. Where there is an occasional early onset of freshet (defined as spring snowmelt derived runoff), variability as defined by the IQR color map is coincident with peak freshet. The persistence of this variability occurs for several months and declines considerably in July and August. There is a remarkable absence of variability overwinter due to the lack of melt events and predictable lack of flow due to ice. Krycklan exhibits similar patterns to Wolf Creek, yet with greater variability in summer and autumn flows, a longer open-water season and more variability in the onset of snow accumulation. The timing of the melt freshet in late April/early May increases variability in flows, which persist over several weeks, yet is less dominant in the overall variability regime compared with Wolf Creek. Late summer flow variability is considerable due to frontal and convective storms. Between mid-December and early April, there is little variability as midwinter melt events are rare.

[28] For Dorset, much of the variability is associated with the spring melt freshet, and a secondary wetting period in October/November which coincides with late-season frontal and tropically derived rainfall on wet soils during a period of reduced evapotranspiration. Snow cover is established by 1 December in most years, yet occasional midwinter melt in January introduces variability that does not occur later in winter due to the persistence of cold temperatures prior to snowmelt.

[29] Periods of variability at Hubbard Brook are much less well defined than at Dorset, with the spring melt freshet the most consistent pattern between the two sites. The summer and early autumn months show less variability with lower flows, although low flows are punctuated periodically during the summer by rain storms causing some variability that does not provide strong signals in the IQR color map. Beginning in September and lasting into early January, runoff increases and becomes more variable with large runoff events that equal the freshet response, generating variability at weekly to longer scales on the color map, reflecting the longer-term nature of this persistent variability. Year-to-year during this period, streamflow is driven by rainfall on wet soils due to reduced evapotranspiration or the onset of snowfall and the reduction of the streamflow response due to freeze up. Consistently cold temperatures in February and March reduce flows and variability, but this pattern reverses at the onset of melt in late March. Compared with the other eastern North American catchments, Hubbard Brook is more responsive to large rainfall events, which occur often during snow-free months.

[30] Sleepers River has a similar variability regime to Dorset, and to a lesser extent Hubbard Brook. Like Dorset, it has a less flashy response with fewer high flow events

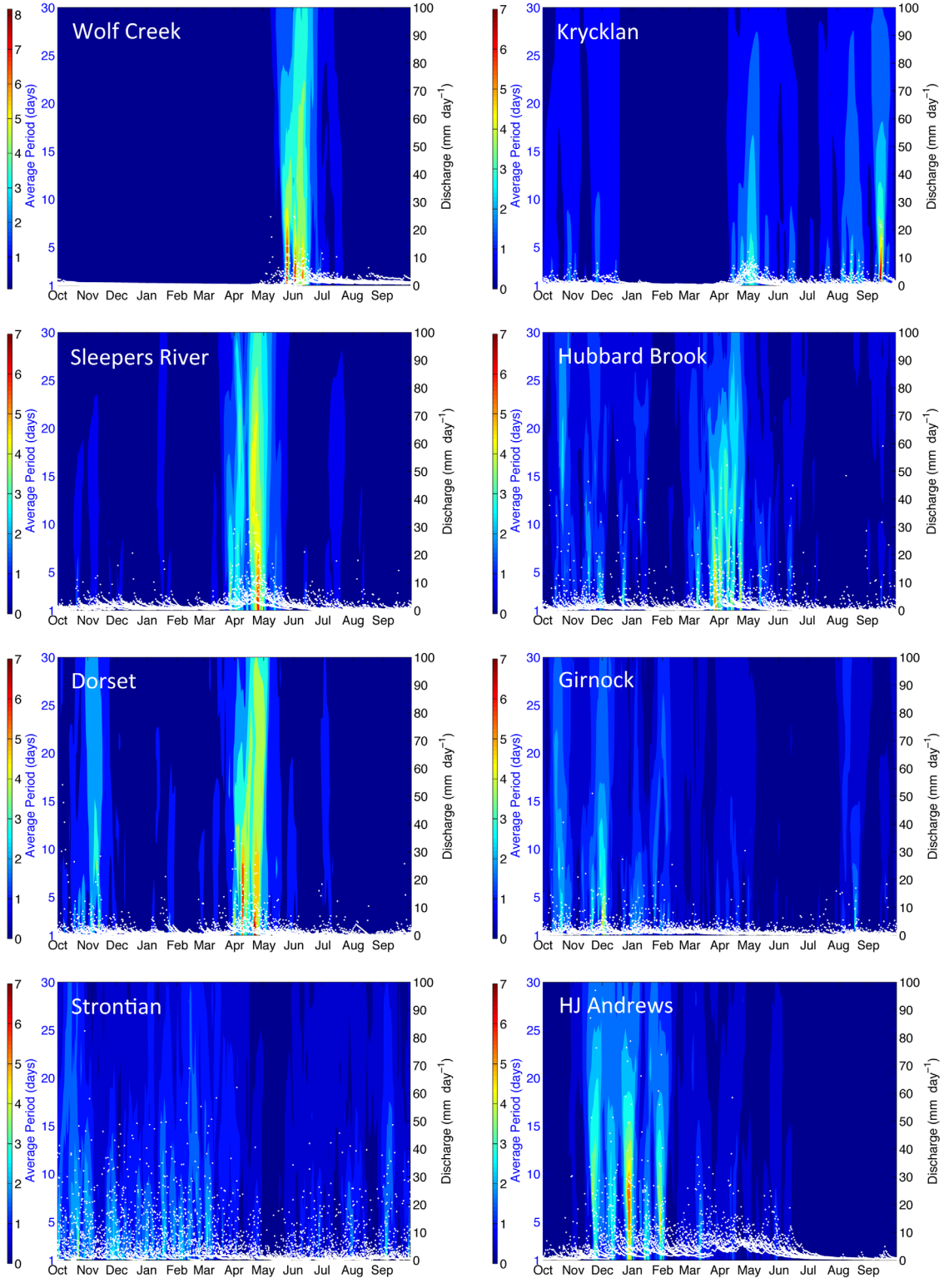

Figure 4. Color maps of flow normalized interquartile range of flow. The left *y* axis shows the averaging period and average flows are shown with white dots (10 years of flow on each day, see right *y* axis for scale). The color depth shows the interquartile range divided by global 10 year mean flow.

that increase variability as at Hubbard Brook. Variability declines in June following melt and increases in early summer when sporadic rain events generate high flows. Variability then gradually declines through early October when the catchment begins to wet up and base flow increases after senescence and leaf-fall. At Sleepers River, enhanced flow and variability may occur through the fall and winter due to frontal storms and winter thaws. Yet like

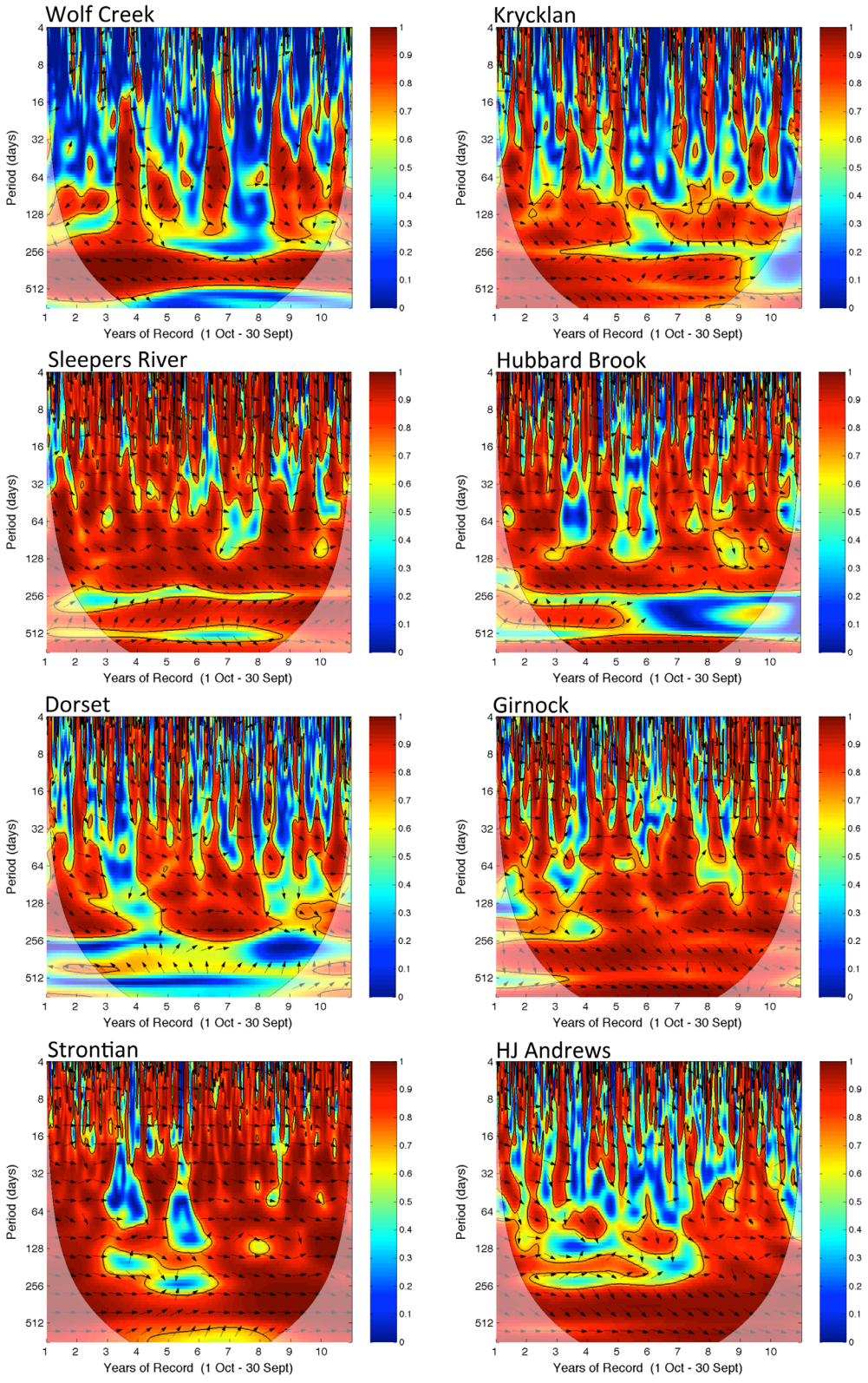

Figure 5. Squared wavelet coherence between precipitation and discharge for 10 years of record. Horizontal axis is the 10 years of record beginning 1 October. Arrows indicate the phase difference between P and Q of the wavelet spectra (right arrows indicate series are in phase, left arrows indicate series are completely out of phase (180°), and an arrow pointing vertically upward means the second series lags the first by 90° (i.e., the phase angle is 270°). Thin solid lines indicate the cone of influence outside of which paler colors indicate the influence of edge effects and must be viewed with caution. Thicker lines bounding areas of red indicate significant coherence at the 95% level against red noise.

Dorset and Hubbard Brook, variability is reduced during the cold period in February and March.

[31] The pattern of variability in Girnock is distinct from those catchments dominated by snowmelt. Precipitation is usually greatest between October and January and then distributed evenly during the remainder of the year (Figure 2). This results in greater flow variability throughout the autumn and winter period, as both rainfall and occasional snowmelt contribute to flow. There is generally little variability in flows between May and September, with the exception of rainfall-runoff events that result in occasional spikes in daily flows that quickly return to base flow levels and are not seen on the color map.

[32] Strontian is wet most of the year, with only a period in May where flows are low and precipitation more limited. There is a persistent variability that is distributed fairly equally throughout the year, with a slight increase in winter flow variability compared with summer. The exception to this variability in May is markedly consistent in each of the 10 years. The implication is that with the exception of this short period, any day of the year has an approximately equal chance of having high or low flow as the dispersion of flows is the closest to uniform among the catchments.

[33] HJ Andrews exhibits the largest seasonal variability in P (Figure 2), with an extremely wet winter and dry summer. Once precipitation declines in June, flows recede to a consistent base flow that exhibits remarkably little variability from late June to late October. As precipitation increases in autumn, flows respond approximately 1 month later as the catchment overcomes a storage deficit and becomes responsive [*Sayama et al*., 2011]. Following this, large frontal events can cause rain, rain-on-snow, or snow-only events that are distributed fairly evenly throughout the wet season. There is a period in February/March when flows are high, yet cold temperatures inhibit melt and substantive addition of water to the soil, thereby limiting variability.

4.2. Wavelet Coherence

[34] The precipitation (rainfall + snowmelt) and runoff wavelet coherencies (Figure 5) can be interpreted as for the 10 years of record; at what period (in days) does coherency occur between the P and Q series. The Cone of Influence (light line) defines areas in full color that are not influenced by edge effects of the wavelet spectra. Colors indicate the strength of the coherence, with orange and red areas within the black lines significant at the 95% level against red noise. Directions of the arrows indicate the degree to which the P and Q series are in phase. Right arrows indicate P and Q are completely in phase, left indicate P and Q are completely out of phase (180° phase angle), and down arrows indicate Q lags precipitation by 90° (one fourth of the cycle at that period). Of all catchments, Wolf Creek, as the driest catchment, shows the weakest coherency between P and Q as evidenced by the large areas that do not show significant coherence between P and Q, although strong coupling occurs at the annual time scale likely due to the large synchronous annual cycles of P and Q. However, there is very weak coherency for most periods at short time scales (4–16 days); the exception being every year midsummer when the catchment is wet following melt and rainfall generates a rapid flow response. The right arrows further support this

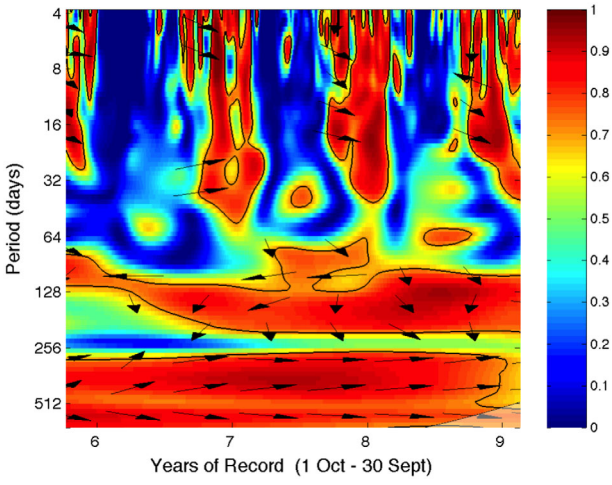

Figure 6. Close-up of squared wavelet coherence between precipitation and discharge for Krycklan for ∼3 years of record. For interpretation of figure, see Figure 4.

rapid runoff generation at this time as P and Q are in phase during this short period. This coherence quickly weakens as soils dry and the thawed zone deepens prior to freeze-back. The influence of snowmelt is observed at approximately 30 days period in most years (offset from the shorter time scale coupling), reflecting the gradual release of the stored snowpack water. At this period of inspection, Q lags P as arrows begin to point down indicating a lag in P and Q signals. This is consistent with long-term field observations in this catchment where much of the catchment has become snow free while flows continue to rise in response to hillslope drainage [*McCartney et al*., 2006].

[35] Krycklan, like Wolf Creek, has coupling at shorter time periods between June and September, which is better observed by closer inspection of ∼3 years of data at higher frequencies (Figure 6). Again, winter flows recede regardless of small inputs, decoupling the P-Q signal. At longer time periods (>1 month), this coupling does identify the freshet melt event. The strongest P-Q coherency occurs at ∼6 months for all years, yet the signals are not directly in phase, identifying that Q cycles lag those of P by ∼3 months when observed over longer time periods. At the annual period, coherence is weaker as P and Q are not always correlated, which is attributed to the influence of catchment storage [*Carey et al*., 2010].

[36] Hubbard Brook, Dorset, and Sleepers River have similar wavelet coherency spectra; coupled largely in the summer/autumn and decoupled in the winter at shorter time scales. There are subtle differences among these catchments, as the wetter Hubbard Brook and Sleepers River have much greater coherency among years and at different temporal scales than Dorset. At Hubbard Brook and Sleepers River, coupling occurs across periodic components from 4 days to 1–4 months for much of the year. Shorter period decoupling occurs in winter and during dry late-summer periods. In contrast, Dorset is drier and has much less coupling, particularly in the later period of record at shorter (submonthly) time periods, reflecting the change in the flow regime (Figure 3). All three catchments exhibit strong coherence at scales of ∼6 months reflecting

seasonal cycles with the phase angles showing the lag offset between P and Q. At the annual scale, Sleepers River and Hubbard Brook show greater coherence, whereas Dorset does not. Decoupling at the annual scale for Dorset may be due to the greater coverage of wetlands and the resultant increase in storage capacity.

[37] Strontian is rainfall dominated, being wet most of the year with a slightly drier period in May that results in P and Q being well synchronized. The catchment exhibits the greatest degree of P-Q coherence of any site across all years and temporal scales. When examining periods without coherency, such as the 1–2 month scale in year 5 and the 4 month scale in years 3 and 8–9, inspection of the P-Q data reveals times when P does not generate a notable streamflow response. The data suggest that large precipitation events do not produce typical P-Q oscillations after longer dry periods, decoupling the signals and resulting in periods without coherence. At shorter time periods (<2 weeks), decoupling is most prevalent during drier summer months. Unlike other catchments, the phase angles suggest the P and Q cycles are much more in phase across all periods, highlighting the responsive nature of this catchment when wet due to limited storage capacity.

[38] P-Q coherency is perhaps most complex at Girnock. This catchment does not have strong wet/dry seasons, nor does snowmelt play a major role in most years. Coupling at short time periods (<1 month) can occur during virtually any time of the year with phase angles suggesting P and Q signals intermittently in phase or slightly lagged. While on balance coupling is greater in winter months, there are periods in each season when P and Q are coupled and decoupled. Periods of strong decoupling appear as vertical blue regions, and are most associated with dry periods. Coherency is strong at the 2–3 month period for most years and for the annual period. Phase angles for this period are offset, demonstrating the lag between P and Q cycles.

[39] HJ Andrews has the greatest variability between wet and dry conditions. Each year, P and Q are strongly coupled from short to monthly time scales for wet fall/winter months (September through March). Beginning each spring, P and Q become decoupled as flows begin a consistent gradual recession from June through September. During this period, small amounts of precipitation do not produce a runoff response, a pattern that is remarkably similar interannually. Again, arrows gradually change from right to down (90° or 1/4 cycle offset) with increasing time period.

5. Discussion

[40] Considering the inherent noise in hydrological systems, and faced with new issues such as nonstationarity in long-term hydrological time series [*Milly et al.*, 2008], there exists a need to explore alternative methods of data analysis and visualization to understand the basis of catchment functioning; particularly during an era of marked environmental change. Northern catchments are thought to be considerably more sensitive to change than temperate catchments as phase change and energy are first-order controls on storage and runoff processes [*Quinton and Carey*, 2008]. Understanding the nature of variability and coupling and how they respond to seasonal and short-term climate patterns provides insight into how catchments may respond to climate variability and their potential susceptibility to change. Color maps (Figure 4) provide an indication of the magnitude and persistence of variability in flows as influenced by short-term and seasonal events. Wavelet coherency (Figure 5) aids in identifying times and the period during which precipitation is coupled/synchronized with discharge, and when integrated with the color maps and process understanding, provides enhanced insight into similarities and differences among the North-Watch catchments.

[41] There are several techniques that can be used to establish persistence or memory in a system, such as spectral techniques that identify dominant temporal/spatial patterns and geostatistical techniques such as semivariograms which identify the relationship between adjacent values. The approach of color-mapping variability (as expressed by the interquartile range) as presented in Figure 3 is an alternate approach for visualizing variability characteristics of flow along with the absolute values, and in a comparative framework can be used to separate the influence of catchment properties from climate forcing. Among the North-Watch catchments, those dominated by snowmelt and strong seasonal cycles in P have the strongest pattern of flow and variability controlled by climate. For example, the pattern of flows and variability in Wolf Creek, which is underlain predominantly with permafrost soils, is controlled largely by the timing of freshet and subzero conditions. Winter recession exhibits almost no variability as midwinter melts do not occur. At the opposite end of our climate gradient, HJ Andrews with well drained and deep soils also has a strong climate-controlled memory from the marked wet and dry season that results in all flow variability occurring from December through June in response largely to rainfall, followed by a period of recession and little flow variability. While both catchments have very different soils and geology, the strong seasonal climate almost completely controls variability in flows. In contrast, Strontian has little intra-annual variability along with thin soils, and with the exception of early May, almost any day of the year can have a high Q in response to a P event. Between these end-members, the remaining North-Watch catchments show some degree of similarity in the nature of flow variability related to climate and snowmelt cycles. Comparison of color maps among the eastern North America catchments suggests that Hubbard Brook is much more responsive with less catchment storage controls on mediating flow variability than Sleepers River and Dorset. At Hubbard Brook, soils have a very tight densipan C horizon at ~0.7 m, limiting deeper percolation and rapidly translating water to the stream through shallow pathways [*Detty and McGuire*, 2010], whereas Sleeper River has well-documented permeable soils [*Dunne and Black*, 1970] that act to mediate flows and variability. Of the three eastern North America watersheds, Dorset has the greatest portion of wetland soils (~13%) and the shallowest relief, which as catchment characteristic dampens the response to precipitation.

[42] When applied to the 10 year precipitation and runoff series, wavelet coherency identified the times at which short (weekly to monthly) and longer-term (monthly to annually) coherence occurred between the P and Q time series. The patterns that emerge from the coherence analysis show both similarities and contrasts, and can be helpful in understanding the predominant mechanism or processes

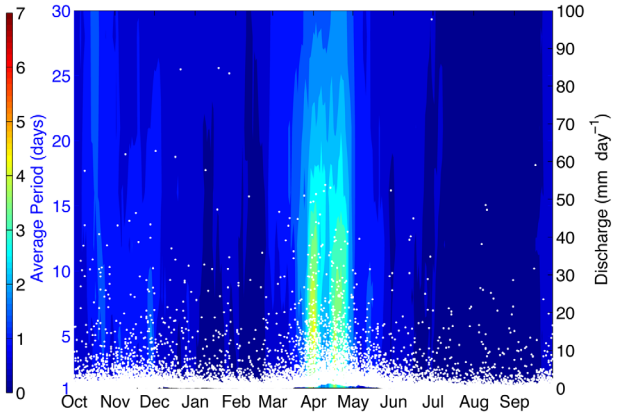

Figure 7. Interquartile range color map for Hubbard Brook of 49 years of discharge data. The left *y* axis shows the averaging period and flows are shown by the white dots (49 points for each calendar day) plotted on the right *y* axis. The color depth shows the interquartile range divided by global 49 year mean flow.

that are occurring at different times. At all sites, short-term coupling occurs during periods of enhanced precipitation and responsive streamflow. For example, almost all snow-dominated sites show coherency at scales from 4 days to 2 months during and immediately after the spring melt period. These patterns are strongest in Krycklan, Hubbard Brook, and Sleepers River, where wet catchments and/or thin responsive soils promote immediate response to precipitation. In catchments with more storage and/or less precipitation, such as Dorset and Wolf Creek, short-term coupling is less well developed as lags occur between input and output response. Wolf Creek is underlain by discontinuous permafrost, and only areas with permafrost soils convey water to the stream during freshet. Hence, much of the catchment can be experiencing melt without a response in streamflow for several weeks [*McCartney et al*., 2006]. At HJ Andrews and Girnock, short-term coupling occurs only during the wet season. At Strontian, short-term coupling occurs more frequently due to the thin soils and large, evenly distributed rainfall events. As scales increase beyond that of a month, catchments exhibit similar behavior with some notable patterns. At a period of 3 or 4 months, most catchments show coherency related to the seasonal signals of P and Q, reflecting the wet/dry cycles in precipitation and runoff. There are notable periods of noncoherence at several sites at these intermediate scales. Inspection of the hydrometric records for Strontian, Hubbbard Brook, and Wolf Creek during "disconnected" periods suggests that the catchments become unresponsive to precipitation events until soil water storage increases after periods of sustained drying (Figure 3). There is a lack of sufficient record length to make this analysis robust at longer periods, but again, inspection of the data shows that wet years do not necessarily result in high runoff years in certain catchments.

[43] Here we have presented an alternate way of visualizing flow variability and applied wavelet coherence analysis to assess coupling. While results provide enhanced insight into catchment function particularly if coupled with process knowledge, there are shortcomings to the analysis and several areas where caution should be exercised. (1) We have analyzed only 10 years of flow data based on data availability. The color maps would exhibit different patterns as more data are introduced into the analysis, or if a different 10 year period is evaluated, particularly for the short-term transient events. As an example, color maps of 49 years of data for Hubbard Brook (Figure 7) show trends that are consistent with those obtained from the 10 year record examined in Figure 3. It would also be possible to use color maps to assess changing flow and variability regimes for different period of interest, allowing for assessment of changing hydrological regimes from external divers. Furthermore, the wavelet analysis would be strengthened with additional years of data, but the overall patterns would likely remain with longer-term signals becoming identifiable assuming the scale range is preserved. (2) There is a flow bias when plotting IQR, even when normalized for mean flows. Similar color maps of coefficient of variation present a different picture, highlighting most strongly periods when low flow variability occurs [*Tetzlaff et al*., 2013]. It is suggested that color mapping of different metrics of variance be explored depending upon the hydrological pattern of interest. (3) The degree-day factor of 4 mm/°C may be less appropriate for cold snowpacks where detailed accounting of energy is more critical for estimating the timing of melt. As a result, the subtleties of coupling P and Q are lost if more precise measure of melt (and P) was obtained. By using the degree-day method, there is a reinforcement of seasonal signals in coherence at the expense of shorter period coherence that would typically occur during periods of low flow. This leads to some inevitability in coherence of P and Q during the postmelt period. (4) Wavelet coherency does not reveal processes, yet similarities in patterns among catchments. It is possible that similar coherence patterns be created from entirely different processes operating within the watershed. As such, caution is required when comparing coherence diagrams among catchments and they have limited utility defining catchment characteristics. (5) We have examined catchments ranging in scale from 0.41 to 30 km^2, which may affect patterns of P-Q coupling as larger catchments are expected to have a greater dampening and storage affect due to longer travel times and channel storage effects. The precise effect of scale on wavelet coherence and color map patterns has not been assessed, and would best be explored under a similar climatic regime with nested catchments of different scales.

6. Conclusions

[44] The overall goal of this paper was to explore the nature of runoff variability among the North-Watch catchments and assess the scales of coupling between precipitation and runoff. This work furthers that of *Carey et al*. [2010] which classified the same catchments based on monthly and annual flow and climate metrics along with topography and storage data. Ten year daily data sets for the catchments were explored using color maps of standard deviation. While color maps are not new [i.e., *Meko et al*., 2012], to our knowledge, there have been no reported applications of color maps to explore the nature of flow variability. While not at first intuitive, the plots highlight the importance of both short-term transient events such as

summer convective storms versus longer-term climate influences (snowmelt, persistent low-pressure periods) for flow variability.

[45] Wavelet coherence was used to explore the coupling of P and Q at different temporal scales for a 10 year period of record. Results showed similar patterns among sites with common drivers of hydrological processes. In catchments with cold winters, P and Q became decoupled during the snow-covered season, yet were strongly coupled during and immediately following the spring freshet. In all catchments, coupling at shorter time scales occurred during wet periods when storage deficits were at a minimum and the watershed was responsive. At longer scales, coupling reflected the coherence between seasonal cycles, being greater at sites with strong seasonal signals.

[46] Although exploratory in nature, this catchment intercomparison exercise further highlights the importance of climate and the 0°C isotherm in the functioning of northern catchments. Despite strong differences in their physical properties, there are common climate drivers that control P-Q coupling and flow variability. The large asynchrony in precipitation, particularly in snow-dominated catchments where inputs are mediated by temperature, dominates the nature of flow variability and P-Q coupling. Under a warming climate, shifts in the timing and magnitude of snowmelt will act distribute flow variability throughout the year and reduce the dominance of snowmelt freshet on patterns of P-Q coupling.

[47] **Acknowledgments.** The authors thank the comments of three anonymous reviewers, particularly for the suggestion of color mapping IQR as a robust measure of dispersion. The North-Watch project (http://www.abdn.ac.uk/northwatch/) is funded by the Leverhulme Trust (F/00 152/AG). The authors are also grateful to those individuals and funding agencies who contributed to gathering the data set presented: Iain Malcolm, Markus Hrachowitz, Julian Dawson for their assistance in generating the database for the Mharcaidh, Strontian, and Girnock catchments. Thanks to staff of the Dorset Environmental Sciences Centre (Ontario Ministry of the Environment) for provision of the data. Ric Janowicz of the Yukon Territorial Government is thanked for the Wolf Creek data. The HJ Andrews team would like to thank Rosemary Fanelli, Tina Garland for assistance with data assembly; John Moreau for data collection, and Don Henshaw for data archiving. The USGS water, Energy and Biogeochemical Budgets (WEBB) program is acknowledged. Hubbard Brook is part of the Long-Term Ecological Research (LTER) network, which is supported by the US National Science Foundation. The Hubbard Brook Experimental Forest is operated and maintained by the USDA Forest Service, Northern Research Station, Newtown Square, PA.

References

Ali, G. A., C. L'Heureux, A. G. Roy, M.-C. Turmel, and F. Courchesne (2011), Linking spatial patterns of perched groundwater storage and stormflow generation processes in a headwater forested catchment, *Hydrol. Processes*, *25*(25), 3843–3857.

Archer, D., and M. Newson (2002), The use of indices of flow variability in assessing the hydrological and instream habitat impacts of upland afforestation and drainage, *J. Hydrol.*, *268*(1-4), 244–258.

Bailey, A. S., J. W. Hornbeck, J. L. Campbell, and C. Eagar (2003), Hydrometeorological database for Hubbard Brook Experimental Forest: 1955–2000, *Gen. Tech. Rep. NE-305*, 36 pp., Northeast. Res. Stn., U.S. Dep. of Agric. For. Serv., Newton Square, Pa.

Beven, K. J. (2001), *Rainfall-Runoff Modelling: The Primer*, 360 pp., John Wiley, Chichester, U. K.

Burn, D. H. (2008), Climatic influences on streamflow timing in the headwaters of the Mackenzie River Basin, *J. Hydrol.*, *352*, 225–238, doi:10.1016/j.jhydrol.2008.01.019.

Buttle, J. (2006), Mapping first-order controls on streamflow from drainage basins: The T-3 template, *Hydrol. Processes*, *20*, 3415–3422, doi:10.1002/hyp.6519.

Carey, S. K., et al. (2010), Inter-comparison of hydro-climatic regimes across northern catchments: Synchronicity, resistance and resilience, *Hydrol. Processes*, *24*(24), 3591–3602, doi:10.1002/hyp.7880.

Clausen, B., and B. J. F. Biggs (2000), Flow variables for ecological studies in temperate streams: Groupings based on covariance, *J. Hydrol.*, *237*(3-4), 184–197.

Detty, J. M., and K. J. McGuire (2010), Topographic controls on shallow groundwater dynamics: Implications of hydrologic connectivity between hillslopes and riparian zones in a till mantled catchment, *Hydrol. Processes*, *24*(16), 2222–2236, doi:10.1002/hyp.7656.

Dunne, T., and R. D. Black (1970), An experimental investigation of runoff production in permeable soils, *Water Resour. Res.*, *6*(2), 478–490, doi:10.1029/WR006i002p00478.

Dyrness, C. T. (1969), Hydrologic properties of soils on three small watersheds in the western Cascades of Oregon, *Res. Note PNW-111*, U.S. Department of Agriculture, Forest Service, Pacific Northwest Forest and Range Experiment Station, Portland, OR, 17.

Foley, J. A., A. Botta, M. T. Coe, and M. H. Costa (2002), El Niño-Southern oscillation and the climate, ecosystems and rivers of Amazonia, *Global Biogeochem. Cycles*, *16*(4), 1132, doi:10.1029/2002GB001872.

Gray, D. M., and D. H. Male (Eds.) (1981), *Handbook of Snow: Principles, Processes, Management and Use*, 776 pp., Pergamon, Toronto.

Grinsted, A., J. C. Moore, and S. Jevrejeva (2004), Application of the cross wavelet transform and wavelet coherence to geophysical time series, *Nonlinear Processes Geophys.*, *11*, 561–566, doi:10.5194/npg-11-561-2004.

Guan, K., S. E. Thompson, C. J. Harman, N. B. Basu, P. S. C. Rao, M. Sivapalan, A. I. Packman, and P. K. Kalita (2011), Spatiotemporal scaling of hydrological and agrochemical export dynamics in a tile-drained Midwestern watershed, *Water Resour. Res.*, *47*, W00J02, doi:10.1029/2010WR009997.

Hrachowitz, M., C. Soulsby, D. Tetzlaff, and M. Speed (2010), Catchment transit times and landscape controls—Does scale matter?, *Hydrol. Processes*, *24*(1), 117–125, doi:10.1002/hyp.7510.

Ionita, M., G. Lohman, N. Rimbu, S. Chelcea, and M. Dima (2012), Interannual to decadal summer drought variability over Europe and its relationship to global sea surface temperature, *Clim. Dyn.*, *38*(1-2), 363–377, doi:10.1007/s00382-011-1028-y.

Jones, J. A. (2005), Intersite comparisons of rainfall-runoff processes, in *Encyclopedia of Hydrological Sciences*, edited by M. Anderson, pp. 1839–1854, John Wiley, Chichester, U. K.

Kang, S., and H. Lin (2007), Wavelet analysis of hydrological and water quality signals in an agricultural watershed, *J. Hydrol.*, *338*(1–2), 1–14, doi:10.1016/j.jhydrol.2007.01.047.

Keener, V. W., G. W. Feyereisen, U. Lall, J. W. Jones, D. D. Bosch, and R. Lowrance (2010), El-Nino/southern oscillation (ENSO) influences on monthly NO(3) load and concentration, stream flow and precipitation in the Little River Watershed, Tifton, Georgia (GA), *J. Hydrol.*, *381*(3-4), 352–363, doi:10.1016/j.jhydrol.2009.12.008.

Kirchner, J. W. (2009), Catchments as simple dynamical systems: Catchment characterization, rainfall-runoff modeling, and doing hydrology backward, *Water Resour. Res.*, *45*, W02429, doi:10.1029/2008WR006912.

Kondrashov, D., Y. Feliks, and M. Ghil (2005), Oscillatory modes of extended Nile River records (A.D. 622–1922), *Geophys. Res. Lett.*, *32*, L10702, doi:10.1029/2004GL022156.

Kruitbos, L. M., et al. (2012), Hydroclimatic and hydrochemical controls on Plecoptera diversity and distribution in northern freshwater ecosystems, *Hydrobiologia*, *693*(1), 39–52, doi:10.1007/s10750-012-1085-1.

Labat, D. (2005), Recent advances in wavelet analyses: Part I. A review of concepts, *J. Hydrol.*, *314*(1-4), 275–288, doi:10.1016/j.jhydrol.2005.04.003.

Labat, D. (2008), Wavelet analysis of the annual discharge records of the world's largest rivers, *Adv. Water Resour.*, *31*(1), 109–117, doi:10.1016/j.advwatres.2007.67.004.

Lafreniere, M., and M. Sharp (2003), Wavelet analysis of inter-annual variability in the runoff regimes of glacial and nival stream catchments, Bow Lake, Alberta, *Hydrol. Processes*, *17*, 1093–1118, doi:10.1002/hyp.1187.

Laudon, H., M. Berggren, A. Ågren, I. Buffam, K. Bishop, T. Grabs, M. Jansson, and S. Köhler (2011), Patterns and dynamics of dissolved organic carbon (DOC) in boreal streams: The role of processes, connectivity, and scaling, *Ecosystems*, *14*(6), 880–893, doi:10.1007/s10021-011-9452-8.

Liu, P. C. (1994), Wavelet spectrum analysis and ocean wind waves, in *Wavelets in Geophysics*, edited by E. Foufoula-Georgiou and P. Kumar, pp. 151–166, Academic, New York.

Lyon, S. W., M. T. Walter, P. Gérard-Marchant, and T. S. Steenhuis (2004), Using a topographic index to distribute variable source area runoff predicted with the SCS curve-number equation, *Hydrol. Processes*, *18*(15), 2757–2771, doi:10.1002/hyp.1494.

Maraun, D., and J. Kurths (2004), Cross wavelet analysis: Significance testing and pitfalls, *Nonlinear Processes Geophys.*, *11*, 505–514, doi:10.5194/npg-11-505-2004.

McCartney, S. E., S. K. Carey, and J. W. Pomeroy (2006), Intra-basin variability of snowmelt water balance calculations in a subarctic catchment, *Hydrol. Processes*, *20*(4), 1001–1016, doi:10.1002/hyp.6125.

McGuire, K. J., J. J. McDonnell, M. Weiler, C. Kendall, and B. L. McGlynn (2005), The role of topography on catchment-scale water residence time, *Water Resour. Res.*, *45*, doi: 10.1029/2004WR003657.

McNamara, J. P., D. Tetzlaff, K. Bishop, C. Soulsby, M. Seyfried, N. E. Peters, B. T. Aulenbach, and R. Hooper (2011), Storage as a metric of catchment comparison, *Hydrol. Processes*, *25*(21), 3364–3371, doi:10.1002/hyp.8113.

Meko, D. M., C. A. Woodhouse, and K. Morino (2012), Dendrochronology and links to streamflow, *J. Hydrol.*, *412–413*, 200–209, doi:10.1016/j.jhydrol.2010.11.041.

Mengistu, S. G., I. F. Creed, R. J. Kulperger, and C. G. Quick (2013), Russian nesting dolls effect—Using wavelet analysis to reveal non-stationary and nested stationary signals in water yield from catchments on a northern forested landscape, *Hydrol. Processes*, *27*, 669–686, doi:10.1002/hyp9552.

Milly, P. C. D., J. Betancourt, M. Falkenmark, R. M. Hirsch, Z. W. Kundzewicz, D. P. Lettenmaier, and R. J. Stouffer (2008), Stationarity is dead: Whither water management?, *Science*, *319*(5863), 573–574, doi:10.1126/science.1151915.

Monk, W. A., D. L. Peters, R. Allen Curry, and D. J. Baird (2011), Quantifying trends in indicator hydroecological variables for regime-based groups of Canadian rivers, *Hydrol. Processes*, *25*(19), 3086–3100, doi:10.1002/hyp.8137.

Niedzielski, T. (2011), Is there any teleconnection between surface hydrology in Poland and El Nino/Southern Oscillation?, *Pure Appl. Geophys.*, *168*(5), 871–887, doi:10.1007/s00024-010-0170-4.

Olden, J. D., and N. L. Poff (2003), Redundancy and the choice of hydrologic indices for characterizing streamflow regimes, *River Res. Appl.*, *19*(2), 101–121, doi:10.1002/rra.700.

Ouachani, R., Z. Bargaoui, and T. Ouarda (2013), Power of teleconnection patterns on precipitation and streamflow variability of upper Medjerda Basin, *Int. J. Climatol.*, *33*, 58–76, doi:10.1002/joc.3407.

Peters, N. E., and B. T. Aulenbach (2011), Water storage at the Panola Mountain research watershed, Georgia, USA, *Hydrol. Processes*, *25*(25), 3878–3889, doi:10.1002/hyp.8334.

Quinton, W. L., and S. K. Carey (2008), Towards an energy-based runoff generation theory for tundra landscapes, *Hydrol. Processes*, *22*, 4649–4653, doi:10.1002/hyp.7164.

Richter, B. D., J. V. Baumgartner, D. P. Braun, and J. Powell (1998), A spatial assessment of hydrologic alteration within a river network, *Regul. River Res. Manage.*, *14*(4), 329–340.

Rouyer, T., J. M. Fromentin, N. C. Stenseth, and B. Cazalles (2008), Analysing multiple time series and extending significance testing in wavelet analysis, *Mar. Ecol. Prog. Ser.*, *359*, 11–23.

Sayama, T., J. J. McDonnell, A. Dhakal, and K. Sullivan (2011), How much water can a watershed store?, *Hydrol. Processes*, *25*(25), 3899–3908, doi:10.1002/hyp.8288.

Shanley, J. B., P. Kram, J. Hruska, and T. D. Bullen (2004), A biogeochemical comparison of two well-buffered catchments with contrasting histories of acid deposition, *Water Air Soil Pollut.*, *4*(2-3), 325–342.

Shook, K. R., and J. W. Pomeroy (2011), Memory effects of depressional storage in Northern Prairie hydrology, *Hydrol. Processes*, *25*(25), 3890–3898, doi:10.1002/hyp.8381.

Si, B. C. (2008), Spatial scaling analyses of soil physical properties: A review of spectral and wavelet methods, *Vadose Zone J.*, *7*(2), 547–562, doi:10.2136/vzj2007.0040.

Soniat, T. M., J. M. Klinck, E. N. Powell, and E. E. Hofmann (2006), Understanding the success and failure of oyster populations: Climatic cycles and Perkinsus marinus, *J. Shellfish Res.*, *25*(1), 83–93, doi:10.2983/0730-8000(2006)25[83:UTSAFO]2.0.CO;2.

Spence, C. (2007), On the relation between dynamic storage and runoff: A discussion on thresholds, efficiency, and function, *Water Resour. Res., 43*, W12416, doi:10.1029/2006WR005645.

Swanson, F. J., and M. E. James (1975), Geology and geomorphology of the H.J. Andrews Experimental Forest, western Cascades, Oregon, *Res. Pap. PNW-188*, Pac. Northwest For. and Range Exp. Stn., For. Serv., U.S. Dep. of Agric., Portland, Oreg.

Tetzlaff, D., C. Soulsby, P. J. Bacon, A. F. Youngson, C. N. Gibbins, and I. A. Malcolm (2007), Connectivity between landscapes and riverscapes—A unifying theme in integrating hydrology and ecology in catchment science?, *Hydrol. Processes*, *21*(10), 1385–1389.

Tetzlaff, D., et al. (2013), Catchments on the Cusp? Structural and functional change in northern ecohydrological systems, *Hydrol. Processes*, *27*, 766–774, doi:10.1002/hyp.9700d.

Torrence, C., and G. P. Compo (1998), A practical guide to wavelet analysis, *Bull. Am. Meteorol. Soc.*, *79*(1), 61–78.

Tromp-van Meerveld, H. J. and J. J. McDonnell (2006), Threshold relations in subsurface stormflow: 2. The fill and spill hypothesis, *Water Resour. Res.*, *42*, W02411, doi:10.1029/2004WR003800.

Wilcox, B. P., W. J. Rawls, D. L. Brakensiek, and J. R. Wight (1990), Predicting runoff from Rangeland Catchments: A comparison of two models, *Water Resour. Res.*, *26*(10), 2401–2410, doi:10.1029/WR026i010p02401.

Wörman, A., G. Lindström, A. Åkesson, and J. Riml (2010), Drifting runoff periodicity during the 20th century due to changing surface water volume, *Hydrol. Processes*, *24*(26), 3772–3784, doi:10.1002/hyp.7810.